

Contents

Table of Contents	i
List of Figures	i
List of Tables	ii
0.1 Coupling Nanodiamonds to Optical Antennas	1
0.1.1 Plasmonic Antennas	1
0.2 Antennas	3
0.2.1 Plasmonic Antennas	5
0.2.2 Structure of the Plasmonic Antennas	7
0.2.3 SiV center in a Plasmonic Double Bowtie Antenna	8
Index	11

List of Figures

1	(a) Picture recorded with a commercial high resolution laser scanning microscope. The area shaded in blue represents the photoluminescence scan in image (b). (b) Photoluminescence scan of a 8 $\mu\text{m} \times 13 \mu\text{m}$	3
2	<caption>	4
3	Image of the sample surface of 100 nm wet-milled nanodiamonds spin-coated on an iridium substrate illuminated with diffuse white light. The white bars are the horizontal bars of the cross markers which serve as a coarse orientation on the sample surface, the white dots are nanodiamonds, the big black spot is an artifact.	4
4	5
5	<caption>	7
6	7
7	<caption>	8
8	<caption>	10
9	<caption>	10
10	<caption>	10
11	<caption>	11
12	<caption>	11
13	<caption>	12

List of Tables

0.1 Coupling Nanodiamonds to Double Bowtie Antenna Structures

Optical antennas are very recent devices designed to efficiently convert freely propagating optical radiation into localized energy and vice versa [?, ?, ?, ?]. Leveraging this unique property, integrating SiV centers with optical antennas creates coupled systems with desirable features. These include enhanced photoluminescence emission and the ability to tailor photoluminescence spectra of the integrated emitters. The latter can be achieved by tuning the physical design parameters of the system including antenna geometry and emitter placement.

In this chapter we report on our efforts aimed at enhancing the properties of SiV centers by coupling them to optical double bowtie antennas. To this end we transfer selected nanodiamonds containing SiV centers to the target antenna structure using pick-and-place methods. After successful coupling we investigate the integrated structure experimentally. In addition to that we successfully relate some of our results to theoretical predictions.

In the following we give a short discussion of the most important properties of optical antennas. Then we sketch the actual coupling process and report on the optical properties of the resulting integrated structure.

0.1.1 Plasmonic Antennas

[?] Optical antennas, acting as converters between propagating and localized fields, provide an effective route to couple photons in and out of nanoscale objects. These antennas are the counterparts of conventional radio and microwave antennas and operate in the visible regime (1, 2). Optical antennas have been shown to focus optical fields to subdiffraction-limited volumes (3), enhance the excitation and emission of quantum emitters (4–7), and modify their spectra (8).

A characteristic of antennas is their directed emission and reception. So far, the control of directionality has mainly been pursued by photonic crystal structures (9) and surface-plasmon-based devices (10–12). However, for such structures approaching the nanometer scale diffraction can limit the collimated beaming of light. On the other hand, the interaction of quantum emitters with light is best enhanced with microcavities(13, 14). Compared with these approaches, plasmonic nanoantennas offer a much smaller footprint in an open geometry combining strong subwavelength fields and increased transition rates, together with the prospect of directionality.

[?] from gold, a metal that can develop charge oscillations in its surface layers when excited by optical radiation. These antennas allow visible radiation, which has wavelengths of hundreds of nanometers, to couple into a semiconductor quantum dot only a few nanometers in diameter, and also direct the emission

Good mode-matched antennas reradiate their energy after excitation within a single cycle of the wave. Molecules or quantum dots take nanoseconds or even longer to reradiate their energy. This time scale corresponds to about 1 million oscillations at optical frequencies, and the emission is in all directions.

If an atom, molecule, or quantum dot is placed into the near-field of a metallic nanoantenna (within about 1/50th the wavelength of the emitted radiation), its excited state can radiate photons very efficiently to free space (see the figure, panel B). The quantum emit-

ters can emit a single photon, which can be exploited in quantum optics. Additionally, the nanoantenna can redirect radiation into a defined solid angle in space and impose a specific polarization on it.

The demonstration of the Purcell effect, which is the acceleration of the decay of the quantum emitter caused by impedance matching by the antenna to free space, could also enhance the radiative emission over nonradiative losses

[?] The electro-magnetic antenna, originally referred to as an "aerial," is a transducer between electromagnetic waves and electric currents, and generally operates in the radiofrequency regime. In analogy with the electro-magnetic antenna, we define the optical antenna as a device that converts freely propagating optical radiation into localized energy, and vice versa. The spatial extent of a receiver or transducer is commonly much smaller than the wavelength of radiation, λ , and is typically of the order of $\lambda/100$.

Surface plasmon resonances make optical antennas particularly efficient at selected frequencies. A generic antenna problem is illustrated in Fig. 3. It consists of a transmitter and a receiver, both represented by dipoles p . The antenna is introduced to enhance the transmission efficiency from the transmitter to the receiver. This enhancement can be achieved by increasing the total amount of radiation released by the transmitter, for which the antenna efficiency is a useful figure of merit:

$$\eta = \frac{P_{rad}}{P} \quad (1)$$

where P is the total power dissipated by the antenna, P_{rad} is the radiated power and P_{loss} is the power dissipated through other means, such as by absorption in the antenna. However, the transmission efficiency can also be improved by directing the radiation in the direction of the receiver. The efficiency for this process is represented by the directivity:

$$\eta = \frac{D}{P} \quad (2)$$

where the angles $\hat{\theta}$ and $\hat{\phi}$ represent the direction of observation and $p(\hat{\theta}, \hat{\phi})$ is the angular power density. The combination of antenna efficiency and directivity is referred to as the antenna gain:

$$\eta = \frac{G}{P} \quad (3)$$

By reciprocity, we can interchange the fields and sources in Fig. 3 to give $p_1 E_2 = p_2 E_1$, where E_1 (E_2) is the field of dipole p_1 (p_2) evaluated at the location of p_2 (p_1). A good transmitting antenna is therefore also a good receiving antenna. For a transmitter in the form of a two-state quantum emitter, reciprocity leads to a relationship between the emitter's excitation rate \dot{N}_{exc} and its spontaneous emission rate:

$$\eta = \frac{\dot{N}_{exc}}{\dot{N}_em} \quad (4)$$

Here, the superscript "0" refers to the absence of the antenna and the subscript "1" indicates the polarization state; that is, the electric field vector points in the direction of the $\hat{\theta}$ unit vector. An equivalent equation holds for polarization in the $\hat{\phi}$ direction. Interestingly, excitation in a direction of high directivity allows the excitation rate to be enhanced more strongly than the radiative rate. Another important antenna parameter is the antenna aperture, which is formally the same as the absorption cross-section sigma. Let us consider a dipole-like receiver with a cross-section σ that is not coupled to an antenna. The unit vector in the direction of the absorption dipole axis is denoted as n_p and the incident field at the location of the receiver is E_0 . Once we couple the receiver to an antenna, the field at the receiver increases to E and the cross-section or antenna aperture becomes

$$\eta = \frac{\sigma}{\sigma_0} \quad (5)$$

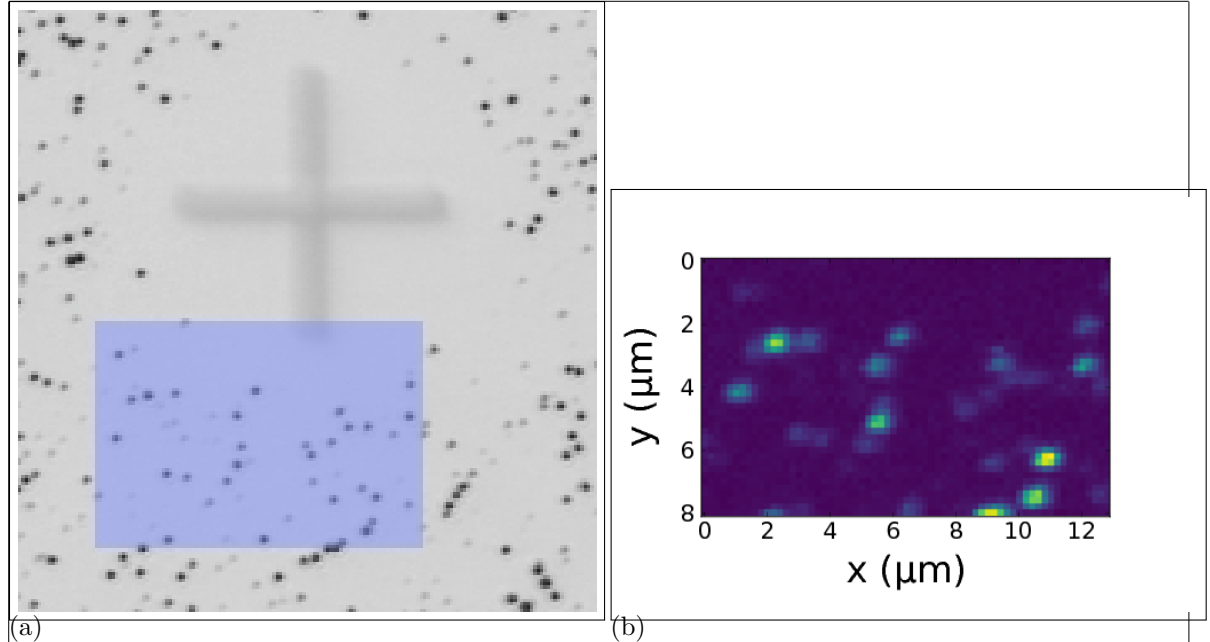


Figure 1: (a) Picture recorded with a commercial high resolution laser scanning microscope. The area shaded in blue represents the photoluminescence scan in image (b). (b) Photoluminescence scan of a $8 \mu\text{m} \times 13 \mu\text{m}$

Thus, the aperture of an optical antenna scales with the local intensity enhancement factor. Theoretical and experimental studies have shown that intensity enhancements of $10^4 \text{--} 10^6$ are readily achievable^{14,36,37} and hence, for typical molecules with free-space^{-1} cross-sections of $\sigma_{\text{mole}} = 1 \text{ nm}^2$, we find that a layer of molecules spaced $0.1 \text{--} 1 \text{ nm}$ apart can absorb all of the incident radiation if each molecule is coupled to an optical antenna. Of course, this estimate ignores the coupling between antennas and therefore has limited validity.

0.2 Coupling Nanodiamonds to Double Bowtie Antenna Structures

In this chapter, the integration of SiV centers in nanodiamonds with double bowtie nanoantenna structures is presented. The emission from the coupled system has two advantages:

- The antenna causes an enhancement in the SiV center's photoluminescence emission intensity.
- The photoluminescence spectrum of the nanodiamond is modified depending on the geometry of the nanoantenna as well as the position of the emitter in the gap. This provides the flexibility of designing the nanoantennas to accurately predict and tune the emitters' PL spectrum as desired.

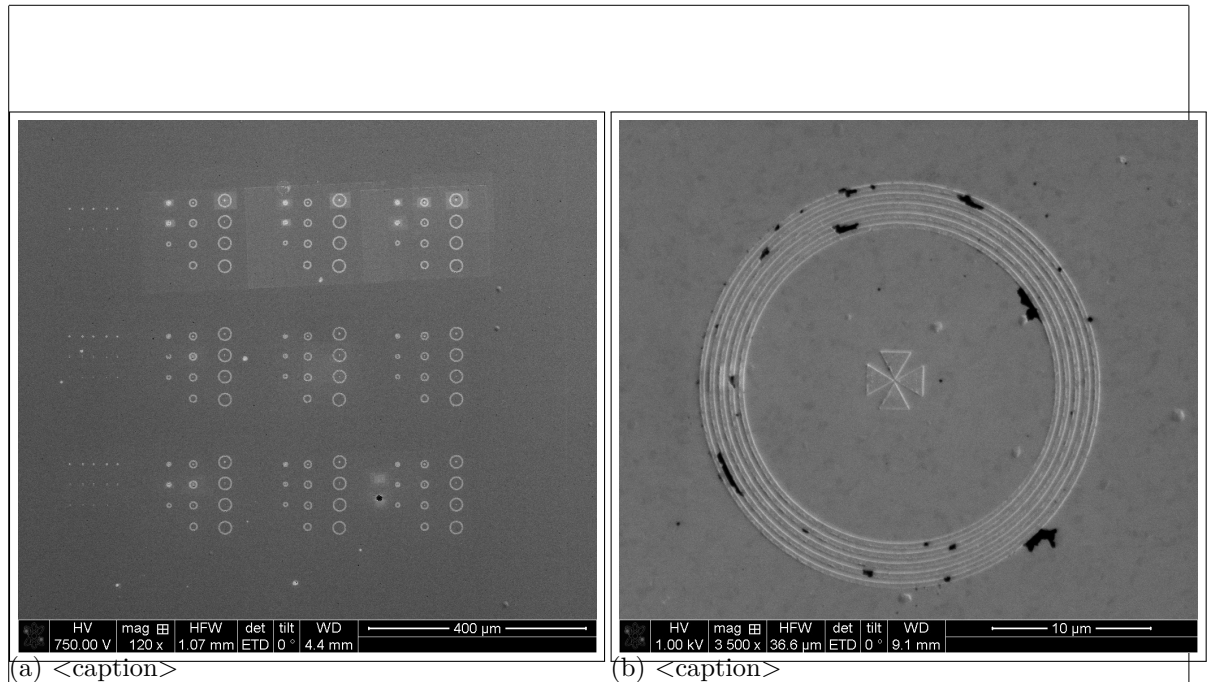


Figure 2: <caption>

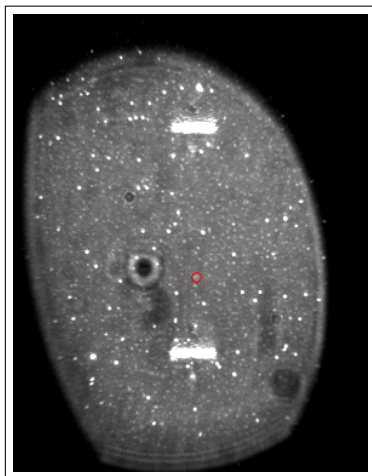


Figure 3: Image of the sample surface of 100 nm wet-milled nanodiamonds spin-coated on an iridium substrate illuminated with diffuse white light. The white bars are the horizontal bars of the cross markers which serve as a coarse orientation on the sample surface, the white dots are nanodiamonds, the big black spot is an artifact.

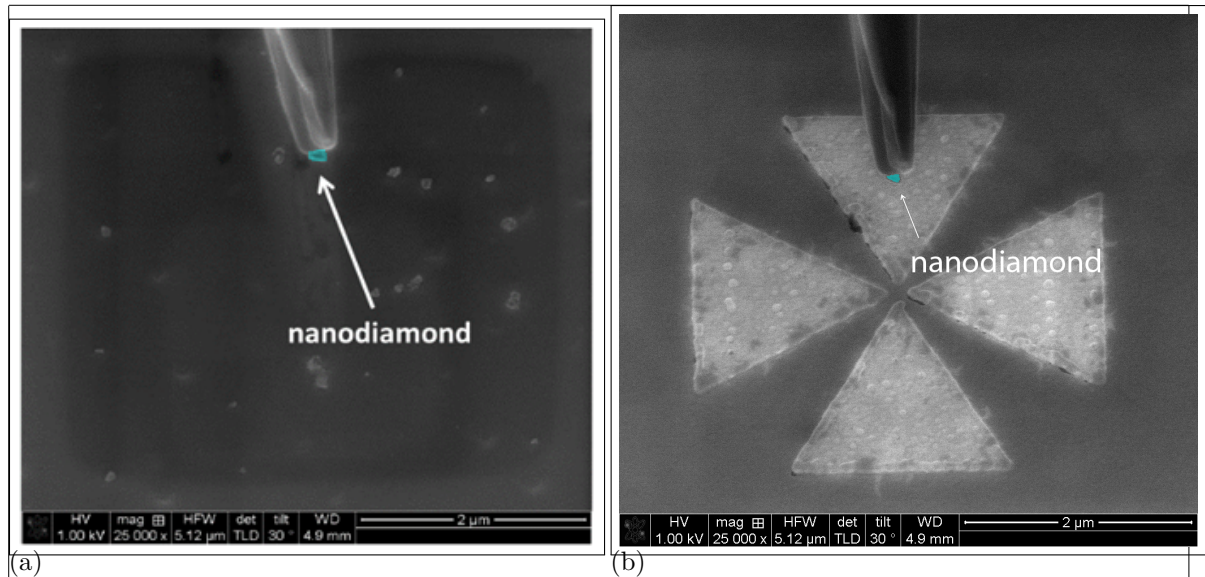


Figure 4

0.2.1 Plasmonic Antennas

[?] Optical antennas, acting as converters between propagating and localized fields, provide an effective route to couple photons in and out of nanoscale objects. These antennas are the counterparts of conventional radio and microwave antennas and operate in the visible regime (1, 2). Optical antennas have been shown to focus optical fields to subdiffraction-limited volumes (3), enhance the excitation and emission of quantum emitters (4–7), and modify their spectra (8).

A characteristic of antennas is their directed emission and reception. So far, the control of directionality has mainly been pursued by photonic crystal structures (9) and surface-plasmon-based devices (10–12). However, for such structures approaching the nanometer scale diffraction can limit the collimated beaming of light. On the other hand, the interaction of quantum emitters with light is best enhanced with microcavities (13, 14). Compared with these approaches, plasmonic nanoantennas offer a much smaller footprint in an open geometry combining strong subwavelength fields and increased transition rates, together with the prospect of directionality.

[?] from gold, a metal that can develop charge oscillations in its surface layers when excited by optical radiation. These antennas allow visible radiation, which has wavelengths of hundreds of nanometers, to couple into a semiconductor quantum dot only a few nanometers in diameter, and also direct the emission.

Good mode-matched antennas reradiate their energy after excitation within a single cycle of the wave. Molecules or quantum dots take nanoseconds or even longer to reradiate their energy. This time scale corresponds to about 1 million oscillations at optical frequencies, and the emission is in all directions.

If an atom, molecule, or quantum dot is placed into the near-field of a metallic nanoantenna (within about 1/50th the wavelength of the emitted radiation), its excited state can radiate photons very efficiently to free space (see the figure, panel B). The quantum emitters can emit a single photon, which can be exploited in quantum optics. Additionally, the

nanoantenna can redirect radiation into a defined solid angle in space and impose a specific polarization on it.

The demonstration of the Purcell effect, which is the acceleration of the decay of the quantum emitter caused by impedance matching by the antenna to free space, could also enhance the radiative emission over nonradiative losses

[?] The electro-magnetic antenna, originally referred to as an "aerial", is a transducer between electromagnetic waves and electric currents, and generally operates in the radiofrequency regime. In analogy with the electro-magnetic antenna, we define the optical antenna as a device that converts freely propagating optical radiation into localized energy, and vice versa. The spatial extent of a receiver or transducer is commonly much smaller than the wavelength of radiation, λ , and is typically of the order of $\lambda/100$.

Surface plasmon resonances make optical antennas particularly efficient at selected frequencies. A generic antenna problem is illustrated in Fig. 3. It consists of a transmitter and a receiver, both represented by dipoles p . The antenna is introduced to enhance the transmission efficiency from the transmitter to the receiver. This enhancement can be achieved by increasing the total amount of radiation released by the transmitter, for which the antenna efficiency is a useful figure of merit:

$$P = P_{\text{rad}} + P_{\text{loss}} \quad (6)$$

where P is the total power dissipated by the antenna, P_{rad} is the radiated power and P_{loss} is the power dissipated through other means, such as by absorption in the antenna. However, the transmission efficiency can also be improved by directing the radiation in the direction of the receiver. The efficiency for this process is represented by the directivity:

$$p = p(\hat{\mathbf{y}}, \hat{\mathbf{T}}) \quad (7)$$

where the angles $\hat{\mathbf{y}}$ and $\hat{\mathbf{T}}$ represent the direction of observation and $p(\hat{\mathbf{y}}, \hat{\mathbf{T}})$ is the angular power density. The combination of antenna efficiency and directivity is referred to as the antenna gain:

$$p = p \quad (8)$$

By reciprocity, we can interchange the fields and sources in Fig. 3 to give $p_1 E_2 = p_2 E_1$, where E_1 (E_2) is the field of dipole p_1 (p_2) evaluated at the location of p_2 (p_1). A good transmitting antenna is therefore also a good receiving antenna. For a transmitter in the form of a two-state quantum emitter, reciprocity leads to a relationship between the emitter's excitation rate \dot{N}_{exc} and its spontaneous emission rate:

$$p = p \quad (9)$$

Here, the superscript "0" refers to the absence of the antenna and the subscript "1" indicates the polarization state; that is, the electric field vector points in the direction of the $\hat{\mathbf{y}}$ unit vector. An equivalent equation holds for polarization in the $\hat{\mathbf{T}}$ direction. Interestingly, excitation in a direction of high directivity allows the excitation rate to be enhanced more strongly than the radiative rate. Another important antenna parameter is the antenna aperture, which is formally the same as the absorption cross-section sigma. Let us consider a dipole-like receiver with a cross-section σ that is not coupled to an antenna. The unit vector in the direction of the absorption dipole axis is denoted as \mathbf{n}_p and the incident field at the location of the receiver is E_0 . Once we couple the receiver to an antenna, the field at the receiver increases to E and the cross-section or antenna aperture becomes

$$p = p \quad (10)$$

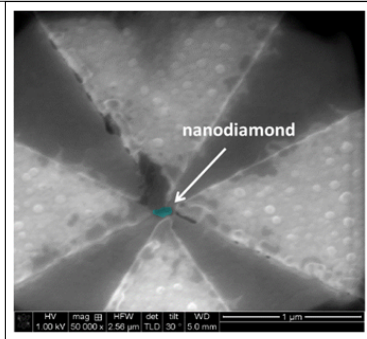


Figure 5: <caption>

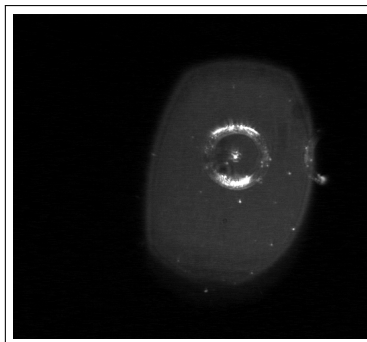


Figure 6

Thus, the aperture of an optical antenna scales with the local intensity enhancement factor. Theoretical and experimental studies have shown that intensity enhancements of 10^4 – 10^6 are readily achievable^{14,36,37} and hence, for typical molecules with π -free-space cross-sections of $\sigma_{\text{mole}} = 1 \text{ nm}^2$, we find that a layer of molecules spaced $0.1\text{--}1 \text{ nm}$ apart can absorb all of the incident radiation if each molecule is coupled to an optical antenna. Of course, this estimate ignores the coupling between antennas and therefore has limited validity.

0.2.2 Structure of the Plasmonic Antennas

FDTD numerical simulations were performed using Lumerical software to characterize gold double bowtie nanoantennas on a gold substrate. The nanoantennas are tailored to have a gap of $g = 150 \text{ nm}$ (taking into account the diameter of the nanodiamonds of around 100 nm), side length of $L = 2 \mu\text{m}$, and a thickness of $t = 60 \text{ nm}$ (see Fig.3a). Upon excitation with incident light, an intense electromagnetic hotspot is formed in the nanoantenna gap [?], which is expected to excite a nanodiamond containing SIV centers aiming to enhance its fluorescence emission. Unlike a single bowtie that is sensitive only to the polarization along its principle axis (C₂ rotational symmetry), a double bowtie features a C₄ rotational symmetry and therefore focuses both parallel and perpendicular polarizations (i.e. all in-plane directions). The index of refraction of gold is taken from Palik [], and that of the nanodiamond is chosen to be $n = 2.4$ at $\lambda = 660 \text{ nm}$. The electric field intensity in the nanoantenna gap is then measured as a function of wavelength to identify the antenna resonance. The spectrum is given in Fig.3b where we observe that the resonance shows two peaks; an intense peak coinciding with the

read paper

Palik, E. D. Handbook of optical constants of solids. 3, (Academic press, 1998)

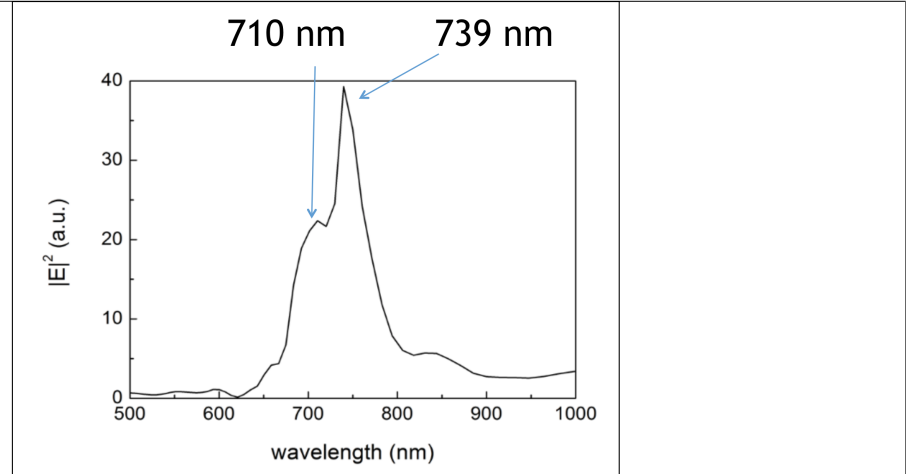


Figure 7: <caption>

SiV emission wavelength ($\lambda = 739 \text{ nm}$), and an additional mode at a lower wavelength ($\lambda = 710 \text{ nm}$) [?]. The resonance spectrum of the antenna alone shows only one peak at 739 nm. Thus, the additional peak is attributed to the presence of the nanodiamond that is slightly shifted from the center of the gap, corresponding to our experimental conditions. These calculations suggest, that the emission from an SiV center at 738 nm is effectively enhanced and directed by the antenna.

0.2.3 SiV center in a Plasmonic Double Bowtie Antenna

In the following, specific details and challenges concerning the coupling process are given and results of the spectroscopic measurements of an SiV center in a plasmonic double bowtie antenna are reported.

We performed coupling the nanodiamonds containing SiV centers in two approaches: First we chose a nanodiamond containing several SiV centers for pick-and-place and afterwards a nanodiamond containing a single SiV center. As mentioned before, single SiV centers may be damaged by the electron radiation in the SEM during pick-and-place and stop emitting photoluminescence light. Hence, we decided to run first experiments with nanodiamonds containing multiple SiV centers. This approach has the advantages that we are able to gain experience in the execution of the pick-and-place process without the risk of permanently damaging the emitter and therefore rendering the tedious pick-and-place process futile. For measurements of the intensity enhancement by the antenna, a single emitter is necessary. However, the antenna's influence on the SiV center spectrum can be studied when several emitters are present. Therefore, studies of the spectrum are performed in this first approach.

After we gained experience with the first approach, we searched for a suited nanodiamond containing a single SiV center. The aim was to perform saturation and second order correlation measurements to probe single SiV centers, and consequently quantify the exact Purcell enhancement imposed by the nanoantenna on a single photon emitter.

Nanodiamond With Multiple SiV centers Coupled to Antenna

The nanodiamonds exploited for the approach of coupling multiple SiV centers to an antenna were produced by a wet-milling process from a CVD diamond film¹. The solution of nanodiamonds which exhibit a median size of 100 nm were spin-coated on an iridium substrate treated with Piranha etch. To ensure that a pre-characterized nanodiamond exhibiting preferred optical properties (eg. narrow linewidth, high count rate) is later found again, the iridium substrate was engraved with reference cross markers produced by a focused ion beam prior to the spin-coating process. After spin-coating, the sample was placed in an oven for 3 hours at 450 °C to oxidize the surface and remove any residual graphite and amorphous carbon.

?? shows the spectrum recorded of the preselected nanodiamond. The ZPL peak exhibits a wavelength of 738.55(1) nm and a linewidth of 5.00(3) nm. These numbers correspond well to the ZPL of unstrained SiV centers and therefore allows us to deduce that the studied nanodiamond contains at least one SiV center. Photon autocorrelation measurements revealed, that the nanodiamond contains multiple SiV centers.

To determine the position of the nanodiamond on the original substrate, first a scan with a commercial laser scanning microscope (LSM) was performed as described in ???. ?? shows a part of an obtained LSM image. The cross marker can easily be identified, the black dots are nanodiamonds. After transferring the sample into the confocal setup, confocal scans of the corresponding areas are performed (??). The area corresponding to the fluorescence light scan in ?? is shaded blue in ???. When looking closely, the bright spots in the fluorescence light scan can be identified with nanodiamonds visible in ???. The image in the SEM is very similar to the image obtained by the LSM. Therefore, once a nanodiamond containing a preselected emitter is identified in the LSM scan, it is easy to find the same emitter in the SEM.

The picking part of the pick-and-place process was performed in the same manner as described in the section about VCSELs (??). The gold surface of the plasmonic antenna caused a high adhesion between the antenna surface and the nanodiamond. Once the nanodiamond touched the gold, it could not be picked up again with the tungsten tip. The nanodiamond first touched the antenna structure a few nanometers away from the gap and immediately stucked to the surface, on top of one of the triangles. Therefore, the nanodiamond had to be pushed into the gap with the nanomanipulator tip. This process caused some damage to the antenna structure. The damage is visible as black area at the tip of the top triangle in ???. However, FDTD simulations of damaged antennas reveal that this modification of the antenna hardly influences the antenna resonance.

After this deterministic placement we measure the PL spectrum of the nanodiamond to identify the effect of the nanoantenna on its emission. The result is displayed in ???. The additional peak at a lower wavelength is attributed to the antenna resonance mode. To verify this, we convolute the experimental PL spectrum of the nanodiamond measured before placing it in the nanoantenna (??) with the intensity spectrum of the nanoantenna obtained by simulations (??). The resulting spectrum is given in ???, and is in good agreement with the measured spectrum in ???, confirming that indeed the extra peak is due to the antenna resonance.

¹wet-milling performed by A. Muzha, group of A. Krueger, Julius-Maximilians Universität Würzburg, diamond film grown by group of O. Williams, School of Engineering, Cardiff University

fehlergrenzen
verfünen
machen

bild dazu

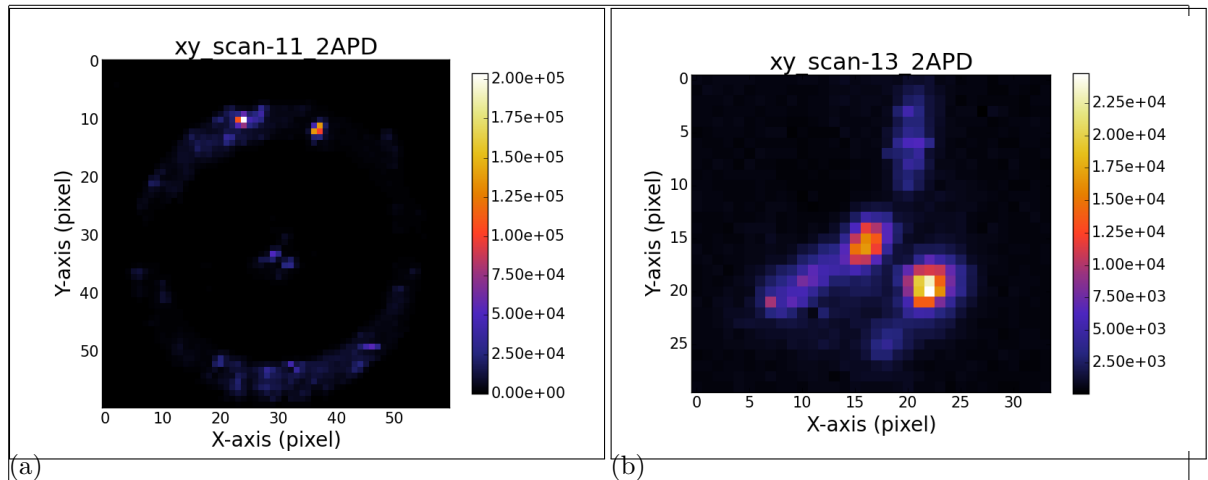


Figure 8: <caption>

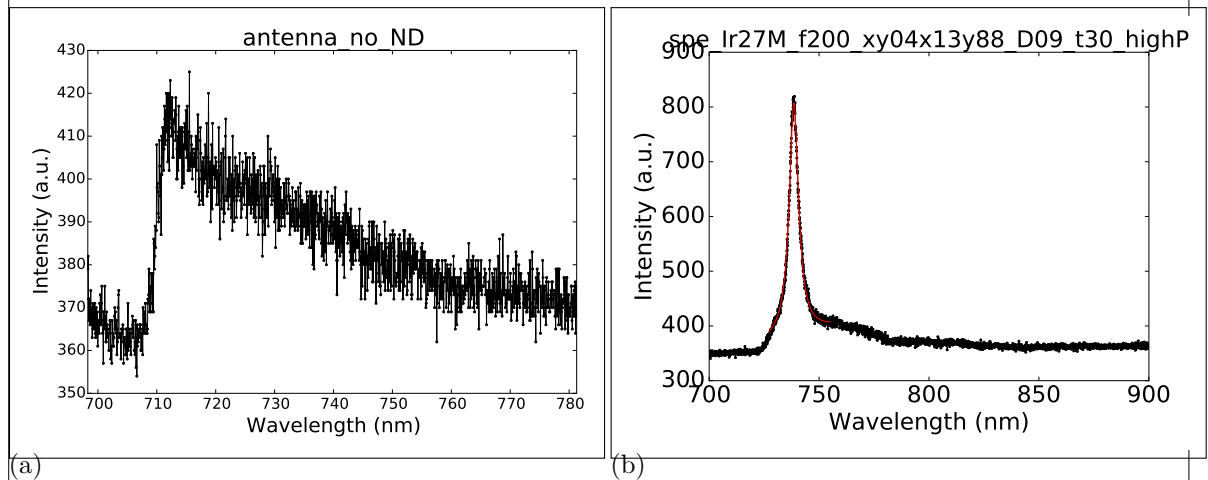


Figure 9: <caption>

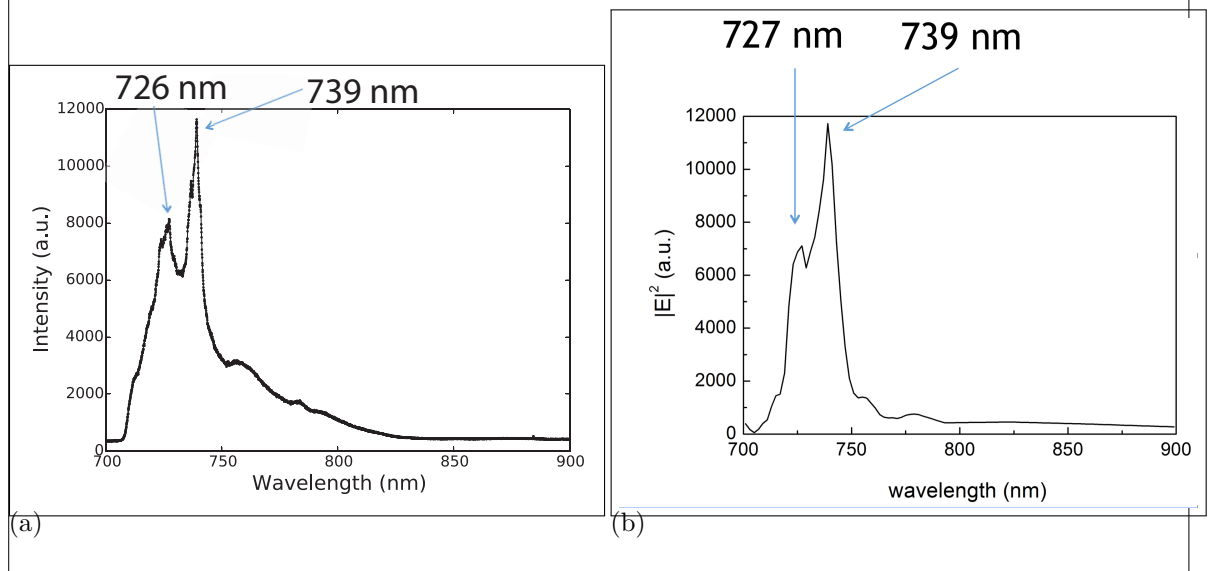


Figure 10: <caption>

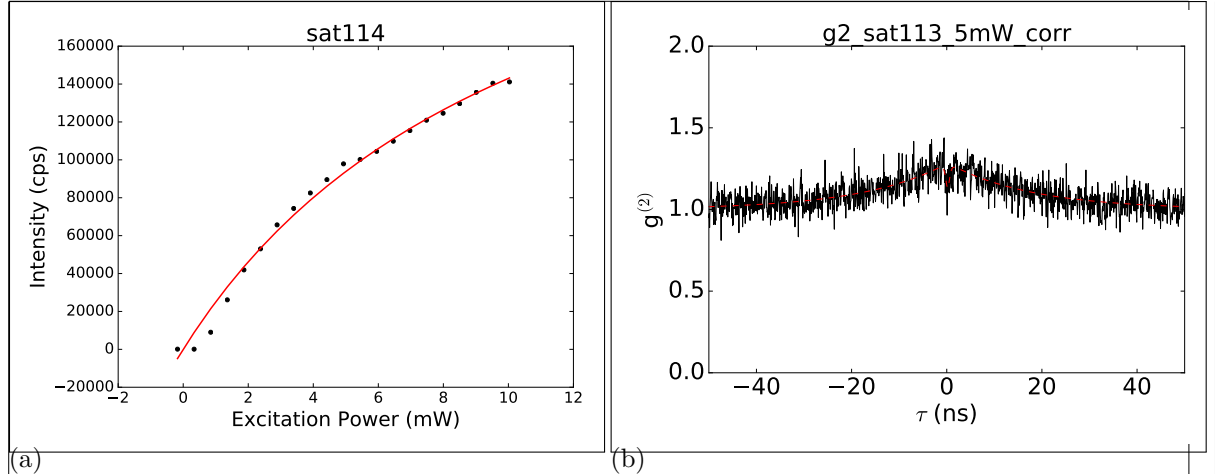


Figure 11: <caption>

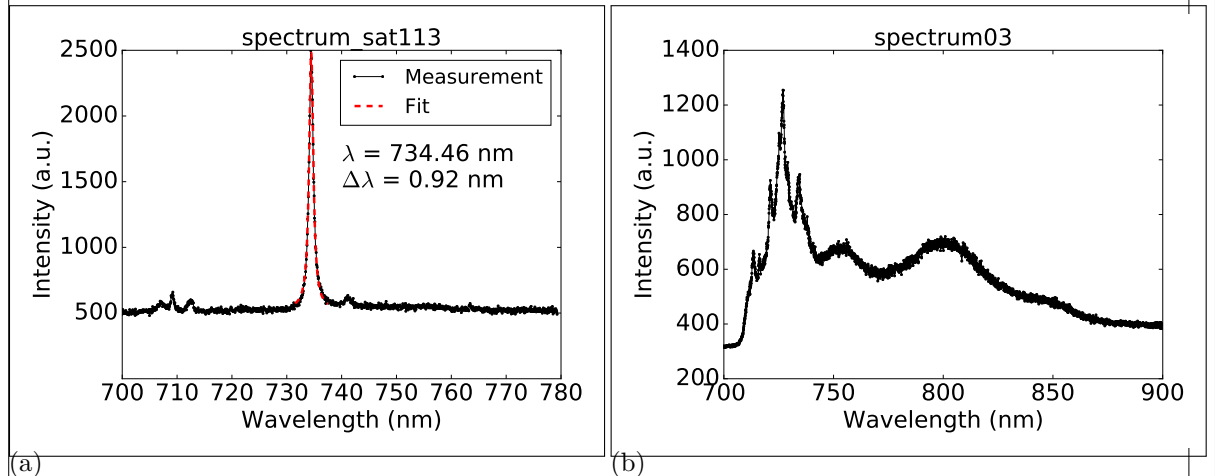


Figure 12: <caption>

Nanodiamond With Single SiV center Coupled to Antenna

sample M02-16: drop-casted with SiGH45 First, only a small percentage of the technically suited nanodiamonds (size, isolation) contain a single SiV center, second, damage due to electron radiation during pick-and-place. After an SiV center with a small dip in the $g^{(2)}$ function, indicating only few SiV centers.

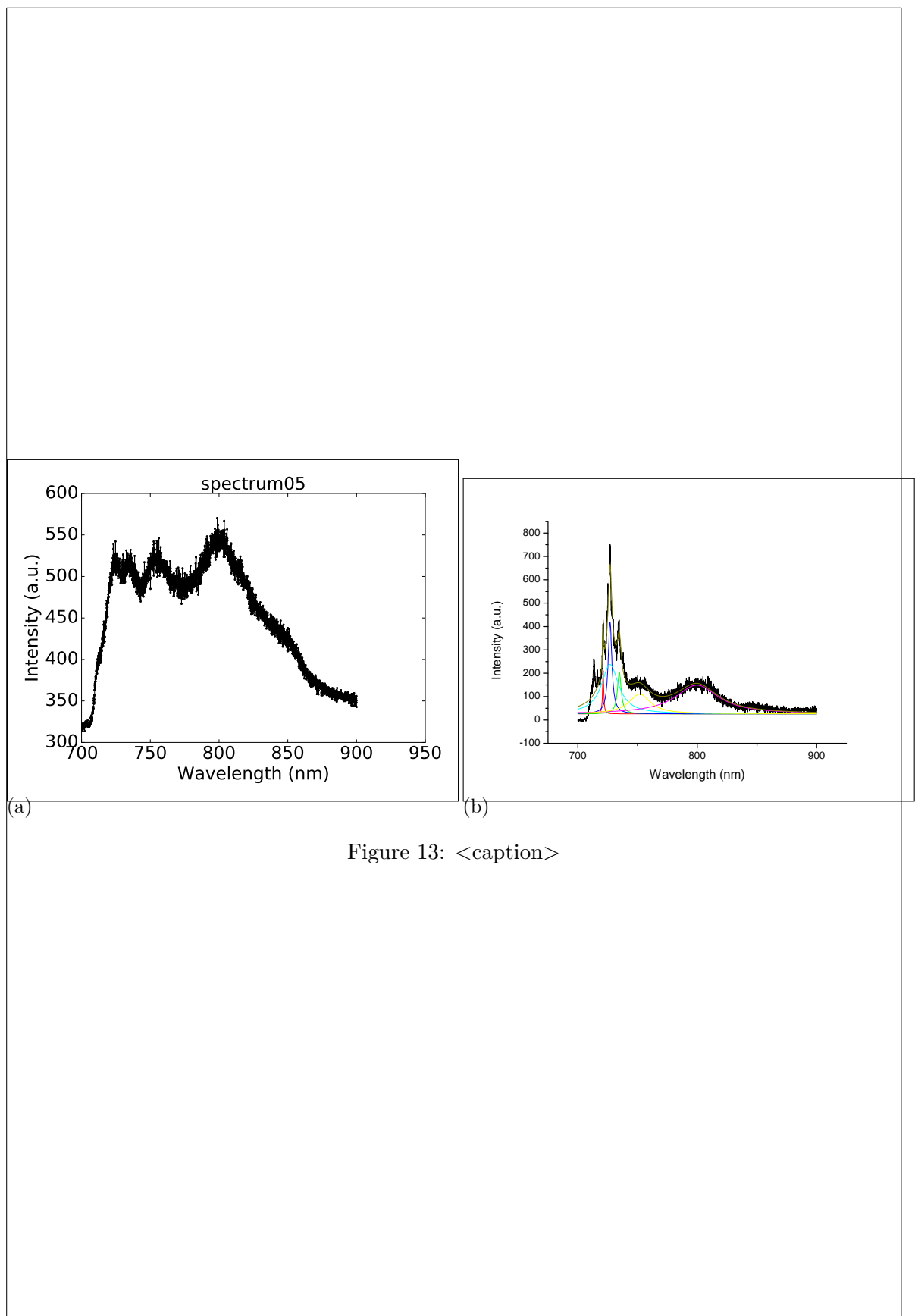


Figure 13: <caption>